Journal of Applied Physics

Temperature dependent electron–phonon coupling of Au resolved via lattice dynamics measured with sub-picosecond infrared pulses

Cite as: J. Appl. Phys. **129**, 193104 (2021); https://doi.org/10.1063/5.0043950
Submitted: 12 January 2021 . Accepted: 11 May 2021 . Published Online: 21 May 2021

John A. Tomko, Sushant Kumar, Ravishankar Sundararaman, and Patrick E. Hopkins

AIP Publishing

Journal of Applied Physics ARTICLE scitation.org/journal/jap

Temperature dependent electron–phonon coupling of Au resolved via lattice dynamics measured with sub-picosecond infrared pulses

Cite as: J. Appl. Phys. **129**, 193104 (2021); doi: 10.1063/5.0043950
Submitted: 12 January 2021 · Accepted: 11 May 2021 ·
Published Online: 21 May 2021

John A. Tomko,[1] Sushant Kumar,[2] Ravishankar Sundararaman,[2] and Patrick E. Hopkins[1,3,4,a)]

AFFILIATIONS

[1]Department of Materials Science and Engineering, University of Virginia, Charlottesville, Virginia 22904, USA
[2]Department of Materials Science and Engineering, Rensselaer Polytechnic Institute, Troy, New York 12180, USA
[3]Department of Mechanical and Aerospace Engineering, University of Virginia, Charlottesville, Virginia 22904, USA
[4]Department of Physics, University of Virginia, Charlottesville, Virginia 22904, USA

[a)]**Author to whom correspondence should be addressed:** phopkins@virginia.edu

ABSTRACT

The detailed understanding of energy transfer between hot electrons and lattice vibrations at non-cryogenic temperatures relies primarily upon the interpretation of ultrafast pump–probe experiments, where thermo-optical models provide insight into the relationship between optical response and temperature of the respective sub-systems; in one of the more studied materials, gold, the Drude model provides this relationship. In this work, we investigate the role of intra- and interband contributions applied to transient optical responses in ultrafast pump–probe experiments using both experiments and first-principle calculations, with probe wavelengths spanning from UV wavelengths into the infrared. We find that during conditions of electron–phonon equilibrium, the Drude model is not applicable to visible wavelengths due to interband transitions. Instead, at probe wavelengths far from these interband transitions (e.g., infrared wavelengths), the optical response is linearly proportional to the temperature of the phonon sub-system and is no longer obfuscated by Fermi-smearing, thus greatly simplifying the extraction of the electron–phonon coupling factor. Our intraband-probe measurements on the electron–phonon coupling factor of Au are in excellent agreement with analytical models and *ab initio* calculations; we observe a constant electron–phonon coupling factor up to electron temperatures of at least ∼2000 K.

I. INTRODUCTION

Energy transfer among out-of-equilibrium particle populations is the fundamental basis for a number of applications where temporally short excitation sources are utilized. Examples range from high-frequency, high-power electronics where electronic relaxation defines the rate of charge transport[1,2] and, at sufficiently high fields, induces dielectric breakdown,[3–5] to photothermal therapies[6,7] and material processing[8,9] with ultrafast sources, where the heat-affected zone is heavily dictated by the rate of which electrons couple to vibrational states. The majority of understanding of these non-equilibrium processes is rooted in the interpretation of ultrafast pump–probe reflectivity measurements. In metals, the relation between non-equilibrium energy transfer rates and the measured optical response is most commonly understood within the framework of the two-temperature model (TTM).[10] In a typical experiment, a sub-picosecond laser pulse excites the electron sub-system to very large temperatures, while the lattice remains cold. Following a time determined by the material's electron–phonon coupling constant, G, these electrons gradually transfer their energy to the material's lattice; the two systems eventually reach equilibrium and diffusive heat transfer processes ensue; a general schematic of this process is shown in Fig. 4(a). The most common method used to interrogate these electron and phonon dynamics during and after sub-picosecond laser heating is through monitoring the reflectivity of a time-shifted probe pulse. The transient change in reflectivity of the probe pulse due to the heating from the sub-picosecond heating event is then assumed to be a measure of the transient temperature changes in the metal. Without

invoking physical models, the probe reflectance change due to these pump-induced temperature excursions is given simply by Ref. 11,

$$\frac{\Delta R}{R} = \frac{R(T) - R(T_0)}{R(T_0)}, \tag{1}$$

where R is the reflectivity prior to excitation at an initial temperature T_0, and $R(T)$ is the probe reflectivity at the excited temperature T. Inclusion of the TTM simply re-states this relationship as a function of the individual temperatures of the electron and phonon subsystems, e.g., $R(T_e, T_p)$. The magnitude of reflectivity change due to these temperature excursions is thus defined by the thermoreflectance coefficients, dR/dT_e and dR/dT_p. Through these relations, one can, in theory, directly relate the measured reflectivity to the temperature transients of the two subsystems.

While the basis of this approach is straightforward, knowledge of these thermo-optic coefficients is crucial toward accurately understanding the non-equilibrium energy transfer dynamics and measuring thermophysical properties such as G. Without *a priori* knowledge of dR/dT_e and dR/dT_p, which are also both wavelength and temperature dependent, it is difficult, if not nearly impossible, to accurately separate these optical coefficients from the thermophysical properties of interest. This issue has led to a large discrepancy in reported values of the electron–phonon coupling factor, G, via pump–probe measurements. In the case of gold, due to its relatively flat density of states around the Fermi energy and its high Debye temperature, one should expect a constant G at elevated temperatures above the Debye temperature, given by Refs. 12 and 13,

$$G = \frac{\pi^2 m_e^* C_s^2 n_e}{6\tau(T_e)T_e}, \tag{2}$$

where m_e^* is the effective mass of the electrons, C_s is the speed of sound, n_e is the electron number density, and $\tau(T_e)$ is the electron relaxation time. In many cases, $\tau(T_e) \sim 1/T_e$, leading to the expectation of a constant G.[14] Regardless of analytical derivations and theoretical/computational studies, many experimental works report a G that is not constant as a function of fluence/electron temperature. Likewise, experiments performed under nearly identical conditions, such as similar electronic temperature excursions, report differing values for G.[15–22] These differences have been hypothesized to be driven by fluence-dependent electron scattering processes in parallel to the electron–phonon interaction, non-thermal relaxation of the excited electron system or steady-state heating that would occur due to pulse accumulation from high repetition rate laser pulses but not in lower repetition rate amplified systems (i.e., measurement artifacts). Clearly, a self-consistent experimental understanding of the role of electron temperature on the electron–phonon coupling factor in gold is missing, leaving theories of electron–phonon coupling in metals during non-equilibrium conditions unverified.

Thus, the questions that we seek to answer in this work are: (i) what is the cause of the wide range of values and discrepancies reported for G of gold? and (ii) how does the electron–phonon coupling factor of gold vary with electron temperature during non-equilibrium conditions when $T_e \neq T_p$?

Most pump–probe systems are based on a visible-to-near infrared lasers, commonly centered at a wavelength of 800 nm. The *static* optical properties of Au at these wavelengths, and most metals, are in fact dominated by free electrons and are well described by the Drude model.[23] Given this, it is commonly, albeit potentially incorrectly, assumed that the pump-induced *change* in optical properties due to temperature excursions lie within this Drude regime. For a given temperature excursion, there are two physical considerations. The first temperature-dependent term in the Drude model is the plasma frequency, defined as

$$\omega_p = \sqrt{\frac{n_e e^2}{m_e^* \epsilon_0}}. \tag{3}$$

While the effective mass, m_e^*, can have a temperature dependence, it is typically negligible for free, intraband electrons. Rather, the number density, n_e, has the most prominent temperature dependence, as it is directly related to the thermal expansion coefficient of the lattice. Note that, e, the charge of an electron, and ϵ_0, the permittivity of free space, are physical constants with no temperature dependence. The second temperature dependence arises in the scattering rate of the free electrons, which is commonly estimated through Matthiessen's rule, $\tau_f^{-1} = A_{ee}T_{ee}^2 + B_{ep}T_p$, where A_{ee} and B_{ep} are constants related to the temperature-dependent electron–electron and electron–phonon scattering rates, respectively.

There are a number of intrinsic flaws associated with this approach. First, while the Drude model applies to near-infrared (NIR) wavelengths under static conditions (e.g., 800 nm), the optical response following short-pulse excitation is strongly dependent on interband transitions under conditions of strong electron–phonon non-equilibrium due to smearing of the Fermi–Dirac distribution at elevated electron temperatures.[24–26] Thus, the Drude model should not be expected to be applicable. Further, the temperature coefficients lack a wavelength dependence, indicating the perturbation of the optical response due to a temperature excursion lacks a wavelength dependence, which is well-known to not be the case. Finally, these scattering coefficients are derived from low-temperature resistivity methods;[27] in the original work where A_{ee} is defined, the coefficient is explicitly defined as not being applicable to radiation frequencies corresponding to visible light.[28]

Recent works have avoided these models, and instead rely on perturbation theory to relate the electron temperature to interpret transient reflectivity data at visible wavelengths;[26] this approach provides one of the more accurate determinations of the electron–phonon coupling factor.[29] In fact, Hohlfeld *et al.* directly monitored the temporal evolution of the Fermi–Dirac distribution in Au following short-pulse excitation, providing a direct measure of the electron temperature. In doing so, they provide a commonly referenced value for the electron–phonon coupling factor ($G = 2.1 \times 10^{16}\,\mathrm{W\,m^{-3}\,K^{-1}}$).[19] While this approach is highly accurate, it is far from straightforward; this approach requires pump–probe data to be acquired at a large number of wavelengths centered about the interband transition of the metal of interest to directly measure the electron temperature. Furthermore, in metals with more complex band structures than that of Au, where multiple electron transitions occur in a small energy range, the ability to

directly relate reflectance to the change in electron distribution can be extremely difficult.[26]

Nonetheless, these inadequacies provide crucial information toward the measurement of electron–phonon interactions via ultrafast pump–probe measurements. As referenced above, the temperature of the phonon subsystem contributes significantly to the transient reflectivity signal and is weakly dependent on wavelength. In the regime of which reflectivity is considered to be intraband in nature, and thus the Drude model is applicable, one obtains a nearly constant thermoreflectance coefficient, which is dominated by the temperature rise of the phonon subsystem. Conversely, the temperature of the electron subsystem and its associated thermo-optic coefficient is strongly dependent on wavelength, due to its strong dependence on interband transitions but trends toward zero at photon energies far from interband transition threshold.[25,26] Given such, we expect that for probe wavelengths far from the interband electronic transitions in a metal, that the thermoreflectance is dominated, if not solely proportional to, the lattice temperature of the metal.

In this work, we investigate the role of interband contributions applied to transient optical responses in ultra-fast pump–probe experiments using both experiments and first-principles calculations. We interrogate the temporal dynamics of ∼20 nm Au on insulating substrates following excitation with a 400 fs, 520 nm pulse using probe wavelengths spanning from 0.85 to 4.35 eV (1500–285 nm) as a means of separating the contributions of the electron and phonon subsystems to the perturbed optical response. Furthermore, we perform *ab initio* calculations to understand the role of intra- and interband contributions to the modulated optical response. In doing so, we find that the electron–phonon coupling factor of Au is in fact constant at least up to electron temperatures of ∼2000 K, consistent with Eq. (2) and free electron theory. In doing so, we posit that the variations in the reported values of G in Au from prior literature could be obfuscated from interband transitions leading to inaccuracies in the thermo-optical model. We summarize an array of reported literature values for the electron–phonon coupling factor of Au as a function of the temperature of the electron subsystem in Fig. 1(b).

II. RESULTS AND DISCUSSION

In excellent agreement with a wealth of literature, we find the ultrafast transient dynamics to be strongly dependent on the probe wavelength in the visible; an example of this observation is shown in Fig. 2. Even in cases of constant pump fluence, ensuring a constant electron–phonon coupling factor, and thus constant temperature transients for the two subsystems, the signals are vastly different for the two probe wavelengths. This observation is traditionally attributed to a variation in thermo-optic coefficients for each wavelength; as the wavelength approaches resonance with an electronic transition, dR/dT_e increases. Indeed, a fit of the TTM to our experimental data demonstrates that dR/dT_e is strongly dependent on the wavelength of the probe, at least for visible wavelengths. Conversely, the phonon-contribution to modulated reflectance,

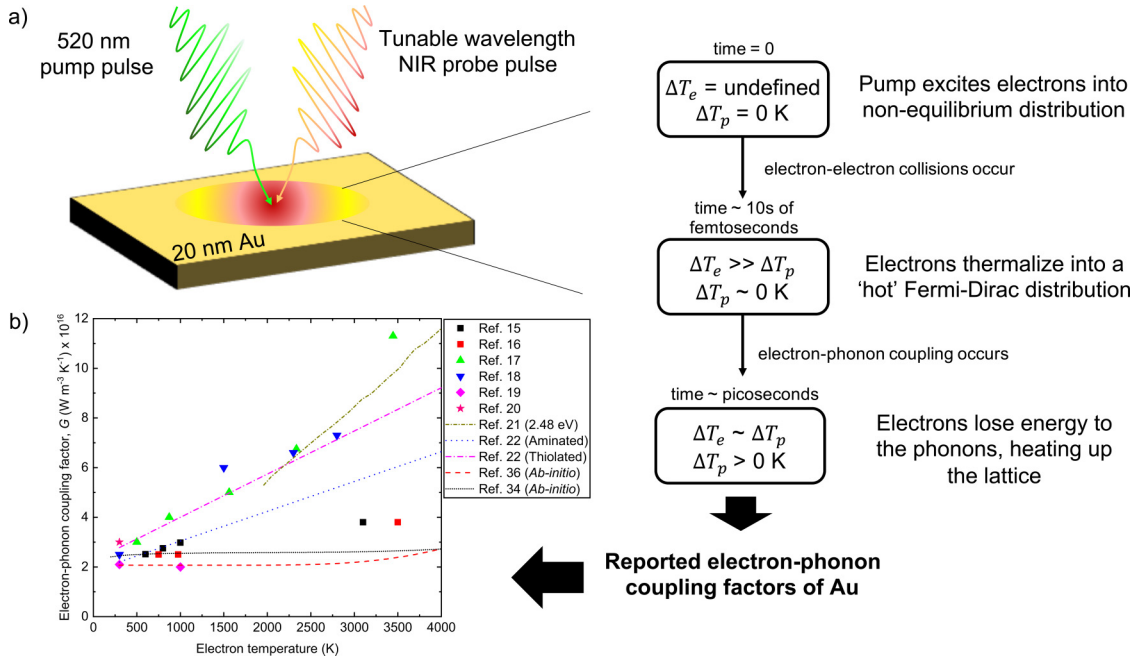

FIG. 1. (a) Experimental schematic of our optical pump–probe measurements on Au (left) and a diagram of the various thermal carrier dynamics following pump excitation in Au (right). (b) Compilation of previous literature values for the measured electron–phonon coupling factor of thin Au films as a function of excited electron temperature are shown as solid symbols, and models and density functional theory calculations are shown as lines. The experimental results are based on ultrafast pump–probe experiments with probe wavelengths in the visible, typically <800 nm.

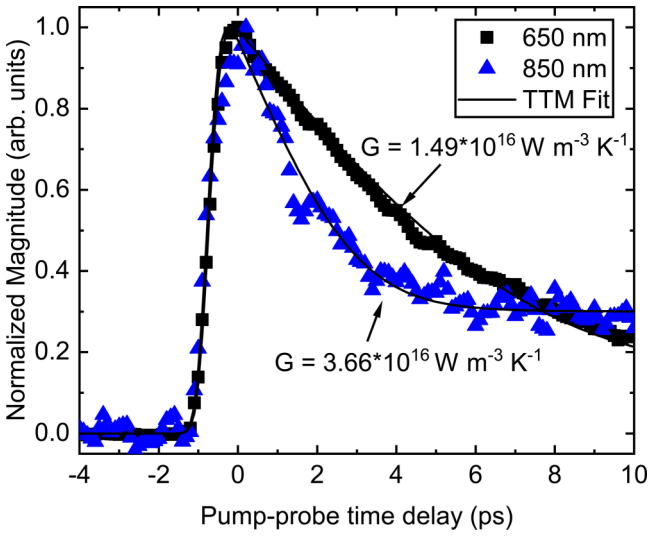

FIG. 2. Experimental data for 20 nm Au films on sapphire substrates at probe wavelengths of 650 nm (black squares) and 850 nm (blue triangles). The pump fluence is approximately 5 J m^{-2} in both cases. Using a perturbed Drude model to relate the electron/phonon subsystems to their respective temperatures yields over a factor of two difference in the calculated electron–phonon coupling factor, even with a constant excitation fluence.

dR/dT_p, is weakly coupled to wavelength. Additionally, at most visible wavelengths, dR/dT_p is found to be orders of magnitude greater in magnitude than dR/dT_e, in agreement with prior works.[11]

To understand the role of interband contributions to thermoreflectance measurements and its effect on interpretation of G, we perform fits of the two-temperature model to our experimental data, acquired as a function of both varying probe wavelength and pump fluences. In these TTM calculations to extract G, we consider three different scenarios of free variables to avoid overfitting. In one case, as done in most prior works, we use literature values for the thermo-optic coefficients, and fit only for the electron–phonon coupling factor (e.g., fit for G, hold dR/dT constant). In the second case, we perform these TTM calculations assuming a constant electron–phonon coupling factor but instead fit for the thermo-optic coefficients (e.g., hold G constant, fit for dR/dT). In the final scenario, we repeat these calculations with both the thermo-optic coefficients and electron–phonon coupling factor as free variables (e.g., fit for both G and dR/dT). We note that the parameters in these TTM calculations are consistent with our previous works[11,30] and values reported in the literature;[31,32] the thermophysical parameters necessary for these calculations can be found in Table I. While most parameters are weakly coupled to temperature, we account for the temperature dependence of the electronic heat capacity via $C_e = \gamma T_e$; the other parameters of interest are validated via time domain thermoreflectance (TDTR) measurements (e.g., the total thermal conductivity of the film and substrate). We additionally note that as the cross-correlation time of the pulses used in our experiments is greater than the timescale of which electrons are

TABLE I. Parameters used for the two-temperature model calculations in this work, where γ is the temperature-dependent coefficient of the electronic heat capacity ($C_e = \gamma T_e$), C_p is the phonon heat capacity, and κ_e and κ_p are the thermal conductivity of the electron and phonon subsystems, respectively. κ_e is determined from four-point probe measurements on our film.

Parameter	Au film	Al_2O_3 substrate
γ (J m^{-3} K^{-2})	68	0
C_p (MJ m^{-3} K^{-1})	2.49	3.06
κ_e (W m^{-1} K^{-1})	135	0
κ_p (W m^{-1} K^{-1})	5	35

non-thermal, we approximate this electron thermalization time as simply an increase in the pulse width. In other words, we utilize an effective pulse width that is the sum of the true pulse duration and the electron thermalization time (e.g., $\tau_{pulse,eff} = \tau_{pulse} + \tau_{ee}$), consistent with prior works.[10,11,33] Note that we utilize this model for the calculation of all electron temperatures referenced in this work. The results of these three fitting procedures to our experimental data are summarized in the following discussion.

As expected, if we fit for both the thermo-optic coefficients as well as the electron–phonon coupling factor, the transient model produced by the TTM is in perfect agreement with our experimental data, however un-physical as this approach may be due to concerns of overfitting. In contrast, if one assumes a constant electron–phonon coupling factor, while fitting for the thermo-optic coefficients, the model fails to capture the experimental data for probe wavelengths close to the interband transition of Au; this approach is found to only show good agreement only for wavelengths above ~700 nm for the fluences used in this work (~1–15 J m^{-2}). Similarly, if one uses thermo-optic coefficients obtained from the Drude model and fit for G, the TTM calculations to deviate greatly from the experimental data as the interband transition is approached; in other words, the TTM fits poorly to the experimental data for this scenario.

To understand the origin of this deviation, we perform *ab initio* calculations of the excitation, relaxation, and time-dependent optical response using the approach detailed in Ref. 34. Briefly, we combine density-functional theory and maximally localized Wannier functions[35] to evaluate contributions of direct interband and phonon-assisted intraband transitions to the carrier distributions (pump excitation) and time-dependent complex dielectric function (probe response) of the metal.[36,37] The hot carrier energy distribution is evolved using the Boltzmann Transport Equation (BTE) with an *ab initio* collision integral including electron–electron and electron–phonon scattering. This parameter-free approach predicts the time-dependent optical response of the metal after pump excitation in quantitative agreement with ultrafast experiments on different plasmonic geometries and materials.[34,38]

The computational framework described above provides the temporal evolution of the complex dielectric function, separated into direct and indirect contributions as

$$\epsilon(\omega, t) = \epsilon_{direct}(\omega, t) + \epsilon_{indirect}(\omega, t), \quad (4)$$

where ω is the frequency of the probe beam. Implementing this dielectric function into the Fresnel equations provides a modulated response given by

$$\frac{dR(\omega, t)}{R(\omega, t)} = \frac{g'(\omega, 0)}{g(\omega, t)}(d\epsilon_{direct}(\omega, t) + d\epsilon_{indirect}(\omega, t)), \quad (5)$$

where g and g' are the electronic density of states before and after optical pump excitation, respectively.

As shown in Fig. 3, we find that interband contributions to the modulated response dominate the optical response at ultrafast timescales for wavelengths less than ~700 nm, invalidating the application of the Drude model to pump–probe data. Furthermore, with increasing fluence, smearing of the Fermi–Dirac distribution leads to a large interband contribution to the modulated response, even for wavelengths initially far from the d-to-s-band transition in Au. Attempting to fit these first-principles results with a TTM leads to similar issues as found in our experimental data; when the interband contribution to the modulated response becomes significant, the perturbed Drude model and/or fitting with a constant G fails.

These first-principles calculations as well as the extrapolation of the wavelength dependence in the thermo-optic coefficients for visible wavelengths elucidate a means to avoid thermo-optical models that are not widely applicable; for probe wavelengths sufficiently far from electronic transitions, the optical response becomes truly free-electron-like. This Drude-like response ultimately lacks sensitivity to the electron temperature and is instead indicative of solely the temperature of the phonon subsystem. Additionally, this free-electron response is linearly proportional to the lattice temperature. This has the advantage of the changes in reflectivity being driven by relatively smaller temperature rises, since the heat capacity of the lattice is orders of magnitude lower than the heat capacity of the electrons. Thus, the non-equilibrium dynamics due to large excursions can be monitored through the much smaller temperature rises of the lattice. In most pump–probe experiments that interrogate these non-equilibrium dynamics of materials in the reversible, non-damage fluence/temperature regime, these lattice temperature rises can be minor and less than a few hundred Kelvin. This greatly simplifies the thermo-optic analysis used in relating the electron and phonon temperature rises to the measured changes in probe reflectivity, in that in this limit of perturbatively small temperature changes, a linear relationship can be assumed between the changes in reflectivity and change in temperature. This linear relationship will remain true for relating $dR(T_p)$ to the lattice temperature rises even during large electron temperature changes where $dR(T_e)$ is a more complex, nonlinear function of T_e.[11]

Therefore, assuming the transient probe thermoreflectance response is in the pure Drude, free-electron regime, the measured change in reflectivity is directly proportional to the temperature evolution of the phonon subsystem, given by

$$C_p \frac{\delta T_p}{\delta t} = \nabla(\kappa_p \nabla T_p) + G(T_e - T_p), \quad (6)$$

where C_p and κ_p are the heat capacity and lattice thermal conductivity of the lattice, respectively. For sufficiently thin films, the thermal conductivity term can be neglected, as the film is homogeneously heated at timescales corresponding to electron–phonon coupling (i.e., the film thickness is less than, or similar to, the optical skin-depth of the pump beam). Thus, in directly monitoring the temperature evolution of *only* the lattice, the exponential rise time in the modulated signal is equivalent to C_p/G.

We experimentally demonstrate this hypothesis at wavelengths far from the interband transition, even following ultrafast excitation, using probe wavelengths in the UV and NIR, corresponding to photon energies of 4.35 and 0.85 eV, respectively. At these wavelengths, the electronic temperature must be in excess of 5000 K to allow interband transitions to affect the optical response of the probe. (While the agreement between IR and UV probes may be somewhat non-intuitive, as the UV photons excite interband transitions on their own, recall that we are measuring the *change* in optical properties of the Au film following pulsed excitation. Thus, the Fermi–Dirac distribution tail must sufficiently smear the d-band electrons to see a change in their initial transition probability.) As shown in Figs. 4(a) and 3, the transient response is vastly different from the typical response at visible wavelengths; there is no presence of a "hot-electron" peak, followed by a decay over a few picoseconds. Rather, there is a clear

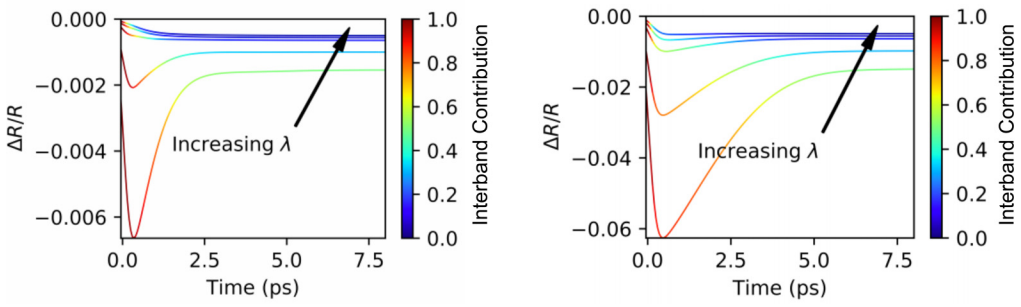

FIG. 3. Relative contribution of direct interband transitions to the probe response of Au at an absorbed fluence of 1 J m^{-2} (left) and 10 J m^{-2} (right) for wavelengths of 600, 700, 900, 1100, and 1300 nm. λ signifies the probe wavelength.

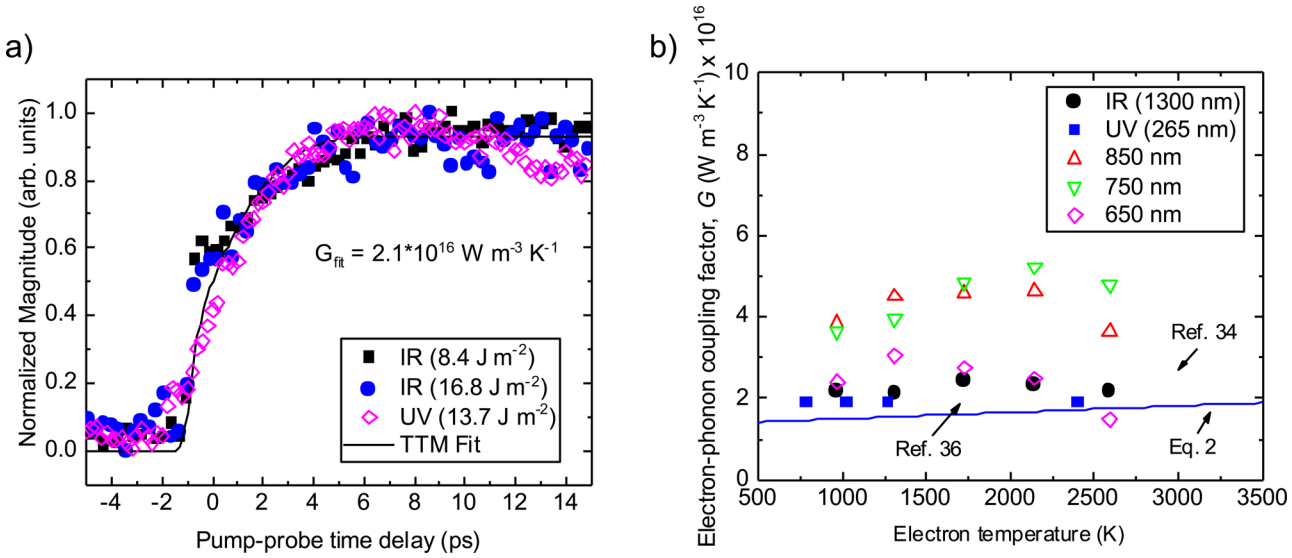

FIG. 4. (a) Experimental pump–probe data at a wavelength of 1300 nm for fluences corresponding to electron temperature rises of ∼1100 K (black squares) and ∼2200 K (blue circles and magenta diamonds) demonstrate the transient reflectivity is dominated by the lattice temperature of the Au, thus eliminating interband contributions. (b) Measured electron–phonon coupling factor from this work's ultrafast pump–probe experiments (symbols), *ab initio* calculations (dashed red and dotted black lines), and calculated from Eq. (2) (solid blue line). At visible probe wavelengths, the measured *G* displays anomalous nonlinearities due to an incorrect application of the Drude model, whereas probe wavelengths that measure far from perturbations of the Fermi–Dirac distribution (e.g., probe via intraband excitations) is relatively constant as a function of electron temperature, up to electron temperatures of ∼2500 K. We find a constant electron–phonon coupling factor that is in excellent agreement with previous works that directly monitor the electron temperature distribution.[19]

exponential rise in the signal, qualitatively similar to the expected increase in lattice temperature following pulsed excitation. Indeed, using the same least squares minimization routine as performed for probe wavelengths in the visible, we find a constant electron–phonon coupling factor for both UV and NIR probes, regardless of fluence. Additionally, the rise time is in excellent agreement with our first-principles calculations. This finding of a constant *G* is in contrast to a number of experimental works, including our own data at visible wavelengths. Nonetheless, the finding of constant electron–phonon coupling factor is in excellent agreement with computational and theoretical approaches for the electron temperatures observed in this work, as well as experimental works that directly monitor the decay of the Fermi–Dirac distribution[19] or the lattice via ultrafast electron diffraction.[39] We attribute the discrepancy between our data far from interband transitions and previous experimental works/our visible data to the assumed relations defining the thermo-optic coefficients at visible wavelengths. We compare our data to an array of literature values for the electron–phonon coupling factor of thin Au films and nanoparticles and show excellent agreement with works that *directly* monitor the electron temperature evolution of Au.[19] Additionally, *G* measured with probe wavelengths far from the smeared Fermi–Dirac distribution is found to be relatively constant, in agreement with both recent *ab initio* calculations,[40] including work[37] that relied on the same computational methodologies described within this work, and analytical formalisms Eq. (2); these data are summarized in Fig. 4(b).

III. CONCLUSION

We demonstrate through a combination of pump–probe measurements with wavelengths spanning UV (285 nm) through the NIR (1500 nm) paired with *ab initio* calculations that the electron–phonon coupling factor of Au is constant up to electron temperatures of at least 2000 K. At wavelengths far from the interband transition of Au, the modulated probe response is dominated by the lattice temperature and allows one to avoid convoluted optical models to interpret the transient response. Additionally, although the *static* optical response of Au can be described through the Drude model, Fermi-smearing invalidates the use of a perturbed Drude model to describe the modulated response for most visible wavelengths. Thus, while more advanced measurement techniques that can directly monitor transient atomic temperatures (e.g., ultrafast diffraction experiments) provide excellent insight into inter-particle scattering and coupling,[39] similar information on the lattice response can be obtained through optical reflectivity measurements, as shown in this work.

Based on the results within, this work elucidates upon the optical regime in which one can perform pump–probe studies to simplify the optical response of Au, which should be easily extended to other metals/materials. In particular, we demonstrate that one can directly interrogate the lattice temperature of metals, without obfuscation of hot electrons, by utilizing probe wavelengths that are sufficiently far from optically induced interband transitions; with any *a priori* knowledge on the band structure of a given metal, the probe wavelength can be chosen to be within this

regime. Further, through comparison of *ab initio* calculations and the wavelength-dependent ultrafast response of metals, the conversion of energy from hot electrons into phonons can be readily understood.[38]

ACKNOWLEDGMENTS

We appreciate support from the Office of Naval Research through a MURI program (Grant No. N00014-18-1-2429). This work was supported in part by the NSF I/UCRC on Multi-functional Integrated System Technology (MIST) Center (Nos. IIP-1439644, IIP-1439680, IIP-1738752, IIP-1939009, IIP-1939050, and IIP-1939012).

The authors declare no conflicts of interest.

DATA AVAILABILITY

The data that support the findings of this study are available from the corresponding author upon reasonable request.

REFERENCES

[1]V. P. Zhukov, V. G. Tyuterev, E. V. Chulkov, and P. M. Echenique, "Electron–phonon relaxation and excited electron distribution in gallium nitride," J. Appl. Phys. **120**, 085708 (2016).
[2]F. M. Abou El-Ela, "Monte Carlo simulation of electron transport in AlGaAs," AIP Conf. Proc. **748**, 86 (2005).
[3]H. Frohlich, "Theory of electrical breakdown in ionic crystals," Proc. R. Soc. A **160**, 230 (1937).
[4]B. C. Stuart, M. D. Feit, S. Herman, A. M. Rubenchik, B. W. Shore, and M. D. Perry, "Optical ablation by high-power short-pulse lasers," J. Opt. Soc. Am. B **13**, 459 (1996).
[5]E. Suzuki, Y. Hayashi, and H. Yanai, "Transport processes of electrons in MNOS structures," J. Appl. Phys. **50**, 7001 (1979).
[6]V. K. Pustovalov, "Light-to-heat conversion and heating of single nanoparticles, their assemblies, and the surrounding medium under laser pulses," RSC Adv. **6**, 81266 (2016).
[7]X. Huang and M. A. El-Sayed, "Gold nanoparticles: Optical properties and implementations in cancer diagnosis and photothermal therapy," J. Adv. Res. **1**, 13 (2010).
[8]S. S. Wellershoff, J. Hohlfeld, J. Güdde, and E. Matthias, "The role of electron–phonon coupling in femtosecond laser damage of metals," Appl. Phys. A: Mater. Sci. Process. **69**, 99 (1999).
[9]M. D. Perry, B. C. Stuart, P. S. Banks, M. D. Feit, V. Yanovsky, and A. M. Rubenchik, "Ultrashort-pulse laser machining of dielectric materials," J. Appl. Phys. **85**, 6803 (1999).
[10]J. K. Chen, D. Y. Tzou, and J. E. Beraun, "A semiclassical two-temperature model for ultrafast laser heating," Int. J. Heat Mass Transf. **49**, 307 (2006).
[11]E. L. Radue, J. A. Tomko, A. Giri, J. L. Braun, X. Zhou, O. V. Prezhdo, E. L. Runnerstrom, J. P. Maria, and P. E. Hopkins, "Hot electron thermoreflectance coefficient of gold during electron–phonon nonequilibrium," ACS Photonics **5**, 4880 (2018).
[12]S. Anisimov, B. Kapeliovich, and T. Perel'Man, "Electron emission from metal surfaces exposed to ultrashort laser pulses," Sov. J. Exp. Theor. Phys. **39**, 375–377 (1974).
[13]M. Kaganov, I. Lifshitz, and L. Tanatarov, "Relaxation between electrons and the crystalline lattice," Sov. Phys. JETP **4**, 173 (1957).
[14]Z. Lin, L. V. Zhigilei, and V. Celli, "Electron–phonon coupling and electron heat capacity of metals under conditions of strong electron–phonon nonequilibrium," Phys. Rev. B **77**, 075133 (2008).
[15]P. E. Hopkins, J. C. Duda, B. Kaehr, X. W. Zhou, C. Y. Peter Yang, and R. E. Jones, "Ultrafast and steady-state laser heating effects on electron relaxation and phonon coupling mechanisms in thin gold films," Appl. Phys. Lett. **103**, 211910 (2013).
[16]A. Giri, J. T. Gaskins, B. F. Donovan, C. Szwejkowski, R. J. Warzoha, M. A. Rodriguez, J. Ihlefeld, and P. E. Hopkins, "Mechanisms of nonequilibrium electron–phonon coupling and thermal conductance at interfaces," J. Appl. Phys. **117**, 105105 (2015).
[17]P. E. Hopkins, J. L. Kassebaum, and P. M. Norris, "Effects of electron scattering at metal-nonmetal interfaces on electron–phonon equilibration in gold films," J. Appl. Phys. **105**, 023710 (2009).
[18]P. E. Hopkins and P. M. Norris, "Substrate influence in electron–phonon coupling measurements in thin Au films," Appl. Surf. Sci. **253**, 6289 (2007).
[19]J. Hohlfeld, S. S. Wellershoff, J. Güdde, U. Conrad, V. Jähnke, and E. Matthias, "Electron and lattice dynamics following optical excitation of metals," Chem. Phys. **251**, 237 (2000).
[20]W. Wang and D. G. Cahill, "Limits to thermal transport in nanoscale metal bilayers due to weak electron–phonon coupling in Au and Cu," Phys. Rev. Lett. **109**, 175503 (2012).
[21]B. Y. Mueller and B. Rethfeld, "Nonequilibrium electron–phonon coupling after ultrashort laser excitation of gold," Appl. Surf. Sci. **302**, 24 (2014).
[22]K. O. Aruda, M. Tagliazucchi, C. M. Sweeney, D. C. Hannah, G. C. Schatz, and E. A. Weiss, "Identification of parameters through which surface chemistry determines the lifetimes of hot electrons in small Au nanoparticles," Proc. Natl. Acad. Sci. U.S.A. **110**, 4212 (2013).
[23]P. B. Johnson and R. W. Christy, "Optical constants of the noble metals," Phys. Rev. B **6**, 4370 (1972).
[24]W. Lu and Y. Fu, *Springer Series in Optical Sciences* (Academic, New York, 2018), Vol. 215, pp. 159–183.
[25]R. W. Schoenlein, W. Z. Lin, J. G. Fujimoto, and G. L. Eesley, "Femtosecond studies of nonequilibrium electronic processes in metals," Phys. Rev. Lett. **58**, 1680 (1987).
[26]T. Heilpern, M. Manjare, A. O. Govorov, G. P. Wiederrecht, S. K. Gray, and H. Harutyunyan, "Determination of hot carrier energy distributions from inversion of ultrafast pump–probe reflectivity measurements," Nat. Commun. **9**, 1853 (2018).
[27]A. H. MacDonald, "Electron–phonon enhancement of electron–electron scattering in Al," Phys. Rev. Lett. **44**, 489 (1980).
[28]M. Kaveh and N. Wiser, "Electron–electron scattering in conducting materials," Adv. Phys. **33**, 257 (1984).
[29]S. D. Brorson, A. Kazeroonian, J. S. Moodera, D. W. Face, T. K. Cheng, E. P. Ippen, M. S. Dresselhaus, and G. Dresselhaus, "Femtosecond room-temperature measurement of the electron–phonon coupling constant in metallic superconductors," Phys. Rev. Lett. **64**, 2172 (1990).
[30]J. A. Tomko, E. L. Runnerstrom, Y. S. Wang, W. Chu, J. R. Nolen, D. H. Olson, K. P. Kelley, A. Cleri, J. Nordlander, J. D. Caldwell, O. V. Prezhdo, J. P. Maria, and P. E. Hopkins, "Long-lived modulation of plasmonic absorption by ballistic thermal injection," Nat. Nanotechnol. **16**, 47 (2021).
[31]A. Block, M. Liebel, R. Yu, M. Spector, Y. Sivan, F. J. García De Abajo, and N. F. Van Hulst, "Tracking ultrafast hot-electron diffusion in space and time by ultrafast thermomodulation microscopy," Sci. Adv. **5**, eaav8965 (2019).
[32]K. Regner, L. Wei, and J. Malen, "Interpretation of thermoreflectance measurements with a two-temperature model including non-surface heat deposition," J. Appl. Phys. **118**, 235101 (2015).
[33]W. M. Ibrahim, H. E. Elsayed-Ali, C. E. Bonner, and M. Shinn, "Ultrafast investigation of electron dynamics in multi-layer metals," Int. J. Heat Mass Transf. **47**, 2261 (2004).
[34]A. M. Brown, R. Sundararaman, P. Narang, A. M. Schwartzberg, W. A. Goddard, and H. A. Atwater, "Experimental and *ab initio* ultrafast carrier dynamics in plasmonic nanoparticles," Phys. Rev. Lett. **118**, 087401 (2017).
[35]I. Souza, N. Marzari, and D. Vanderbilt, "Maximally localized Wannier functions for entangled energy bands," Phys. Rev. B: Condens. Matter **65**, 1 (2002).
[36]A. M. Brown, R. Sundararaman, P. Narang, W. A. Goddard, and H. A. Atwater, "Nonradiative plasmon decay and hot carrier dynamics: Effects of phonons, surfaces, and geometry," ACS Nano **10**, 957 (2016).

[37]A. M. Brown, R. Sundararaman, P. Narang, W. A. Goddard, and H. A. Atwater, "*Ab initio* phonon coupling and optical response of hot electrons in plasmonic metals," Phys. Rev. B **94**, 075120 (2016).
[38]M. N. Su, C. J. Ciccarino, S. Kumar, P. D. Dongare, S. A. Hosseini Jebeli, D. Renard, Y. Zhang, B. Ostovar, W. S. Chang, P. Nordlander, N. J. Halas, R. Sundararaman, P. Narang, and S. Link, "Ultrafast electron dynamics in single aluminum nanostructures," Nano Lett. **19**, 3091 (2019).
[39]M. Z. Mo, Z. Chen, R. K. Li, M. Dunning, B. B. Witte, J. K. Baldwin, L. B. Fletcher, J. B. Kim, A. Ng, R. Redmer, A. H. Reid, P. Shekhar, X. Z. Shen, M. Shen, K. Sokolowski-Tinten, Y. Y. Tsui, Y. Q. Wang, Q. Zheng, X. J. Wang, and S. H. Glenzer, "Heterogeneous to homogeneous melting transition visualized with ultrafast electron diffraction," Science **360**, 1451 (2018).
[40]A. Giri, M. V. Tokina, O. V. Prezhdo, and P. E. Hopkins, "Electron–phonon coupling and related transport properties of metals and intermetallic alloys from first principles," Mater. Today Phys. **12**, 100175 (2020).